View metadata, citation and similar papers at core.ac.uk

brought to you by CORE

provided by Missouri University of Science and Technology (Missouri S&T): Scholars' Mine

Missouri University of Science and Technology

Scholars' Mine

Materials Science and Engineering Faculty Research & Creative Works

Materials Science and Engineering

01 Dec 2008

# Structural Properties and Crystallization of Sodium Tellurite Glasses

Kresimir Furic

Masa Rajic-Linaric

C. S. Ray
*Missouri University of Science and Technology*, csray@mst.edu

A. Šantić

*et. al. For a complete list of authors, see https://scholarsmine.mst.edu/matsci_eng_facwork/122*

Follow this and additional works at: https://scholarsmine.mst.edu/matsci_eng_facwork

 Part of the Materials Science and Engineering Commons

## Recommended Citation

K. Furic et al., "Structural Properties and Crystallization of Sodium Tellurite Glasses," *Croatica Chemica Acta*, Croatian Chemical Society, Dec 2008.

This Article - Journal is brought to you for free and open access by Scholars' Mine. It has been accepted for inclusion in Materials Science and Engineering Faculty Research & Creative Works by an authorized administrator of Scholars' Mine. This work is protected by U. S. Copyright Law. Unauthorized use including reproduction for redistribution requires the permission of the copyright holder. For more information, please contact scholarsmine@mst.edu.

CROATICA CHEMICA ACTA
CCACAA **81** (4) 559–567 (2008)

ISSN-0011-1643
CCA-3275
*Original Scientific Paper*

# Structural Properties and Crystallization of Sodium Tellurite Glasses

**Ana Šantić,[a,*] Andrea Moguš-Milanković,[a] Krešimir Furić,[b] Maša Rajić-Linarić,[c] Chandra S. Ray,[d] and Delbert E. Day[d]**

[a]*NMR Center, Ruđer Bošković Institute, 10000 Zagreb, Croatia*

[b]*Molecular Physics Laboratory, Ruđer Bošković Institute, 10000 Zagreb, Croatia*

[c]*Laboratory for Thermal Analysis, Brodarski Institute, 10000 Zagreb, Croatia*

[d]*Graduate Center for Materials Research, Missouri University of Science and Technology, Rolla, MO 65409, USA*

RECEIVED APRIL 25, 2007; REVISED NOVEMBER 6, 2007; ACCEPTED NOVEMBER 30, 2007

The structural properties and crystallization behaviour of $x$Na$_2$O-(100-$x$)TeO$_2$ ($0 \le x \le 33.3$, $x$-% mole fraction) glasses have been investigated by Raman spectroscopy, X-ray diffraction (XRD) and differential scanning calorimetry (DSC). The Raman spectra of glasses show systematic changes in structural units, from TeO$_4$ trigonal bypiramids (tbps) to TeO$_3$ trigonal pyramids (tps) with increasing Na$_2$O content in glass. These structural changes are result of Te–$_{eq}$O$_{ax}$–Te disruption and the formation of non-bridging oxygens (NBOs) in glass network. When heated at 623 K for 10 h glasses crystallized to different phases: $\alpha$-TeO$_2$, Na$_2$Te$_4$O$_9$ and a new crystalline phase which is believed to be a polymorph of Na$_2$Te$_2$O$_5$.

*Keywords*
tellurite glasses
structure
crystal phases
DSC
Raman spectroscopy

## INTRODUCTION

Tellurite-based glasses are of considerable interest because of their low melting temperature, high refractive index and high transmission in the infrared region.[1–3] They appear to be among the most interesting materials for nonlinear optoelectronic devices due to large third-order nonlinear optical susceptibility. Furthermore, these glasses are considered as very good materials for hosting lasing ions since they provide a low phonon energy environment to minimize non-radiative losses.[4,5]

It is well known that tellurium oxide, TeO$_2$, is a conditional glass-former and can be prepared in glassy state only using very high cooling rates such as roller-quenching[6] or vapor deposition.[7] Besides that, pure TeO$_2$ glass is not stable and crystallizes easily due to the presence of lone pair of electrons at the equatorial position of TeO$_4$ units, which seriously limits the structural rearrangement of these units necessary for glass formation.[8] However, the addition of a small amount of modifier oxides, such as Na$_2$O, makes TeO$_2$ a very good glass-former.

The structure of binary Na$_2$O-TeO$_2$ glasses has been investigated extensively by a variety of experimental techniques,[9-16] as well as theoretical calculations.[17] According to Raman spectra, Sekiya *et al.*[10] have reported that the structure of TeO$_2$ glasses with a small amount of Na$_2$O (up to 20 % mole fraction) is a continuous random

* Authors to whom correspondence should be addressed. (E-mail: asantic@irb.hr)

network of $TeO_4$ trigonal bipyramids (tbps) and $TeO_{3+1}$ polyhedra having one nonbridging oxygen, NBO. In the glasses containing 20–30 % mole fraction of $Na_2O$, with increasing NBOs, the $TeO_3$ trigonal pyramds (tps) are formed in the continuous network. At nearly 50 % mole fraction of $Na_2O$ the glass structure consists of $TeO_{3+1}$ polyhedra and $TeO_3$ tps along with the isolated $Te_2O_5^{2-}$ and $TeO_3^{2-}$ units.

Generally, $Na_2O$-$TeO_2$ glasses show marked stability which is composition-dependent with maximum at ≈ 20 % mole fraction of $Na_2O$.[15,16] The explanation for such a high resistance to devitrification is based on the broad distribution of polyhedra found in these glasses relative to crystals at or near the same compositions.[15] The significance of this distribution is that extensive chemical transformations, not just repacking, are necessary to form crystals from the glasses upon heating.

The crystalline phases in the $x$$Na_2O$-(100-$x$)$TeO_2$ system exist at $x$ = 0 ($\alpha$-$TeO_2$, $\beta$-$TeO_2$, $\gamma$-$TeO_2$, $\delta$-$TeO_2$), $x$ = 20 ($Na_2Te_4O_9$), $x$ = 33 ($Na_2Te_2O_5$) and $x$ = 50 ($Na_2TeO_3$), $x$ being % mole fraction. However, recently Zhu *et al.* have reported the existence of new crystalline phase at $x$ = 11.1 ($Na_2O{\cdot}8TeO_2$, NT8).[7] Similarly, recent investigation undertaken by Holland *et al.* has revealed several new metastable crystalline phases for various compositions of $Na_2O$-$TeO_2$ system which are more closely related to the glass structure than thermodynamically stable crystalline phase.[18]

Despite the numerous investigations, the structural properties and crystallization processes in $Na_2O$-$TeO_2$ glass system are still far from clarity. Therefore, the relationship between structures of $Na_2O$-$TeO_2$ glasses and its crystalline counterparts still remains an interesting area of research. The aim of the present study was to gain further insight into the structure of $x$$Na_2O$-(100-$x$)$TeO_2$ ($0 \le x \le 33.3$ % mole fraction) glasses and their devitrification products using differential scanning calorimetry (DSC), X-ray diffraction analysis (XRD) and Raman spectroscopy. Prepared $x$$Na_2O$-(100-$x$)$TeO_2$ ($0 \le x \le 33.3$ % mole fraction) glasses were crystallized by heating at 623 K for 10 h in air and crystalline phases were analyzed.

## EXPERIMENTAL

The pure $TeO_2$ glass used in the present work was prepared in the form of micron-size (0.5 to 2.0 μm) glass beads by melting and evaporating a 20.0 $Na_2O$ – 80.0 $TeO_2$ % mole fraction glass. A small amount (≈ 40 mg) of the 20.0 $Na_2O$ – 80.0 $TeO_2$ glass contained in a small platinum heating coil (≈ 5 mm long and 2 mm internal diameter) was heated to a temperature of about 1200 K. The melt adhered to the heating coil (by surface tension) started evaporating profusely, and the evaporating species were collected on a glass substrate placed directly on the stream of vapor.

The $x$$Na_2O$-(100-$x$)$TeO_2$ ($x$ = 14.3, 20.0, 25.0 and 33.3 % mole fraction) glasses were prepared by melting an appropriate mixture of $TeO_2$ (99.99 %, Alfa Aesar) and $NaNO_3$ (99.9 %, Aldrich Chemicals) raw materials at 1023 K for 30 min in platinum crucible in air. The melt was quenched between two steel plates to produce a glass plate of about 2 mm thickness. The amorphous character of the glasses was confirmed by XRD. No platinum was detectable in any of these glasses by X-ray fluorescence spectroscopy (XRF), which suggests that the dissolution of platinum from the crucible into the melt was negligible.

The glass transition ($T_g$) and crystallization ($T_c$) temperatures for the glasses were measured by DSC, TA Instruments, DSC Model 2910. The DSC curves were obtained by placing ≈ 50 mg of glass particles, size < 125 μm, in open platinum pan, and heating the particles at 10 K/min, in a nitrogen atmosphere at a flow rate of 100 $cm^3$/min. The estimated error in $T_g$ and $T_c$ is ± 0.5 K.

Each glass was crystallized by heating at 623 K for 10 h in air. The heat treatment temperature was chosen based on the DSC results, Figure 1. Since the first crystallization peaks for investigated $Na_2O$-$TeO_2$ glasses containing minimum (14.3 % mole fraction) and maximum (33.3 % mole fraction) $Na_2O$ content are at 603 and 601 K respectively, it was of interest to examine the formation of crystalline phases due to heating of all glasses slightly above these crystallization temperatures. All glasses were heated for 10 h in order to obtain high degree of crystallinity. Crystalline phases were determined by XRD (Philips PW 1050) using

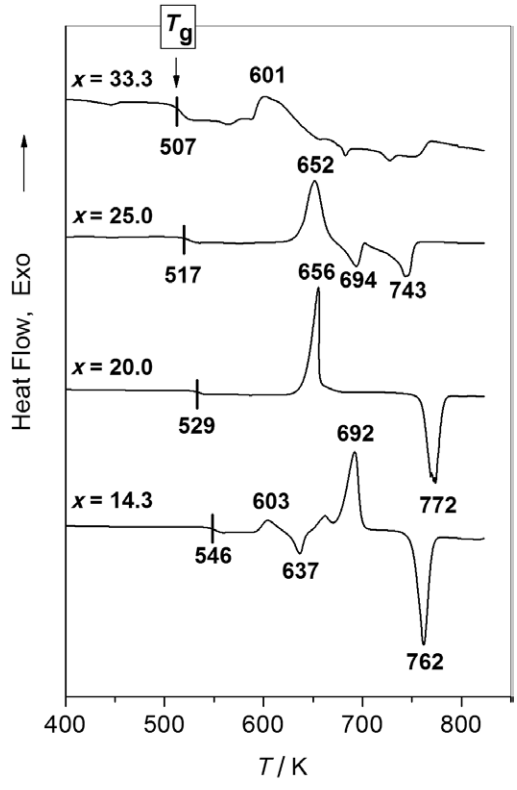


Figure 1. DSC curves for the $x$$Na_2O$-(100-$x$)$TeO_2$ ($14.3 \le x \le 33.3$ % mole fraction) glasses.

nickel Cu-Kα radiation and were identified according to data existing in the Joint Committee on Powder Diffraction Standards (JCPDS).

The Raman spectra of glasses and crystallized samples were obtained using 20 mW of 514.5 nm light from a Coherent argon ion laser (Model Innova 100) and were recorded with a computerized triple monocromator (Dilor Z 24). The digital intensity data were recorded from 10 to 1500 $cm^{-1}$ at intervals of 2 $cm^{-1}$. A 90° scattering geometry was used with the sample oriented at a near-grazing angle. Laser beam 1.5 mm in diameter was focused on the sample using single lens with the focal length of 100 mm. So, the beam diameter at the sample place was 50 μm. Due to the near-grazing geometry, illuminated sample area was elliptic in shape, 50 × 2000 μm. Raman scattered light was collimated using Nicon objective series E with the *f* number *f*/1.8 giving total magnification of 6× between the sample and entrance slit. The Raman spectra were taken at several different spots on each sample in order to investigate homogeneity of the material. The complex shape of the experimentally recorded Raman bands was analyzed by the least squares fitting procedure assuming a Gaussian shape for all bands.

The microstructure and chemical compositions of glasses and crystallized samples were evaluated by SEM (JEOL T300) equipped with energy dispersive X-ray (EDS) detector (Vega TS 5136 Tescan). The nominal composition of the glasses was determined by EDS analysis by analyzing each sample at six different positions.

## RESULTS AND DISCUSSION

### *Pure $TeO_2$ Glass*

It was mentioned above that the pure $TeO_2$ glass can be prepared only conditionally using special fast quenching technique such as roller-quenching[6] or vapor deposition.[7] The $TeO_2$ glass beads in the present study was prepared by vapor deposition from 20.0 $Na_2O$ – 80.0 $TeO_2$ % mole fraction glass. A higher vapor pressure of $TeO_2$ at 1000 K (≈ 1.3 × $10^{-1}$ mm Hg) than that of $Na_2O$ (≈ 1.5 × $10^{-3}$ mm Hg) causes $TeO_2$, not $Na_2O$, to evaporate from this $Na_2O$-$TeO_2$ melt. Analysis by X-ray diffraction (XRD) and energy dispersive X-ray analysis (EDS) confirmed that the species deposited on the glass plate were amorphous particles of pure $TeO_2$, and contained no $Na_2O$.

### *DSC Measurements*

The DSC curves for $x$$Na_2O$-(100-$x$)$TeO_2$ ($14.3 \le x \le 33.3$ % mole fraction) glasses are shown in Figure 1. Each curve contains several exo- and endo-thermic peaks that are characteristics of different transformations, such as glass transition, crystallization and melting. The first small baseline change corresponds to glass transition. The glass transition temperature, $T_g$, decreases consistently from 546 to 507 K with increasing $Na_2O$ content from 14.3 to 33.3 % mole fraction. The values for $T_g$ are in excellent agreement with those reported by Heo *et al.*[11]

For sodium tellurite glass containing 14.3 % mole fraction of $Na_2O$, the DSC curve exhibits three exothermic peaks at 603, 662 and 692 K which reveals crystallization of several phases. The first peak at 603 K perfectly matches peak at ≈ 603 K attributed to crystallization of new phase $Na_2O \cdot 8TeO_2$ in DSC curve for 11.1 $Na_2O$ – 88.9 $TeO_2$ % mole fraction glass.[7] This new $Na_2O \cdot 8TeO_2$ phase is not stable at or above 613 K and readily transforms to $Na_2Te_4O_9$ and $TeO_2$.[7] According to this, the small endothermic peak at 637 K can be related to melting of $Na_2O \cdot 8TeO_2$ phase, whereas exothermic peaks at 662 and 692 K may be attributed to crystallization of $Na_2Te_4O_9$ and $TeO_2$. The large endothermic peak at 762 K is related to complete melting.

The DSC curve for the glass containing 20.0 % mole fraction of $Na_2O$ shows sharp crystallization peak at 656 K indicating crystallization of a single crystalline phase $Na_2Te_4O_9$ as expected from the phase diagram.[19,20] For the glass with 25.0 % mole fraction of $Na_2O$ the DSC curve exhibits broader crystallization peak at 652 K, but the presence of two melting peaks at 694 and 743 K suggests that more than one phase crystallized also from this glass. The DSC curve for the glass containing 33.3 % mole fraction of $Na_2O$ contains a broad asymmetric exothermic peak at ≈ 601 K. This broad shape of the crystallization peak may be attributed to slow process of crystallization through the surface mechanism or simultaneous crystallization of more than one phase. It is well known, that sharp crystallisation peak implies a higher order reaction (bulk, three dimensional growth) while a broad peak signifies a lower order (surface, one dimensional growth) reaction.[21]

### *XRD Analysis*

The $x$$Na_2O$-(100-$x$)$TeO_2$ ($0 \le x \le 33.3$ % mole fraction) glasses were crystallized at 623 K for 10 h in air, and than analyzed by XRD, Figure 2. According to JCPDS data, the diffraction peaks in the XRD pattern of crystallized $TeO_2$ glass free of $Na_2O$, correspond to those for $\alpha$-$TeO_2$ (PDF 42-1365), whereas for crystallized glass containing 14.3 % mole fraction of $Na_2O$ diffraction pattern contains additional peaks related to $Na_2Te_4O_9$ (PDF 32-1166). The crystallization of $\alpha$-$TeO_2$ and $Na_2Te_4O_9$ instead of $Na_2O \cdot 8TeO_2$ phase from the glass containing 14.3 % mole fraction of $Na_2O$ is not unexpected since this glass was heat treated at 623 K which is in the temperature range of decomposition of $Na_2O \cdot 8TeO_2$ phase, Figure 1.

The glass containing 20.0 % mole fraction of $Na_2O$ crystallized to phase $Na_2Te_4O_9$, Figure 2, as expected from the DSC results and phase diagram for $Na_2O$-$TeO_2$ system.[19,20] On the other hand, the XRD pattern for glass

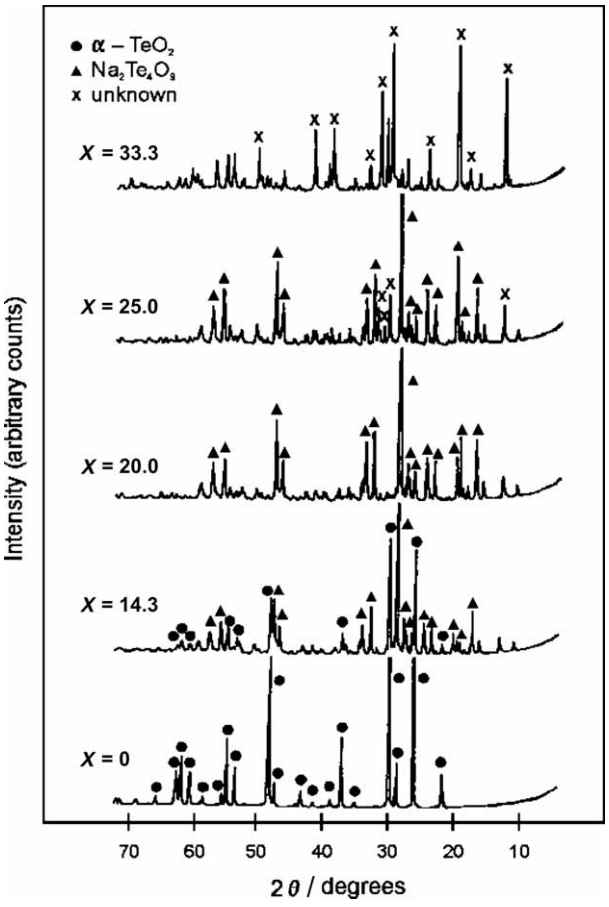


Figure 2. XRD patterns for the $x$Na$_2$O-(100-$x$)TeO$_2$ ($0 \le x \le 33.3$ % mole fraction) crystallized glasses.

with 25.0 % mole fraction of $Na_2O$ contains peaks related to $Na_2Te_4O_9$ and additional unidentified peaks that become dominant in XRD pattern of glass with 33.3 % mole fraction of $Na_2O$. According to phase diagram for the $Na_2O$-$TeO_2$ system, this unknown phase should be $Na_2Te_2O_5$.[20] However, the diffraction peaks for $x = 33.3$ % mole fraction do not match with the peaks for $Na_2Te_2O_5$ or for any other composition (including $Na_2O$-$TeO_2$ phases: $Na_2Te_2O_7$, $Na_4TeO_5$, $Na_2TeO_4$) available in the JCPDS files. Similar XRD pattern has been reported recently by Holland *et al.* for glass of the same composition, 33.3 $Na_2O$ – 66.7 $TeO_2$ % mole fraction heat treated at 558 K for 1 h.[18] According to same authors this phase corresponds to a metastable form of $Na_2Te_2O_5$. Since in the present study, glass of this composition was crystallized at higher temperature (623 K) and for longer time (10 h), it seems that unknown phase shows significant stability in this temperature range.

### *SEM-EDS Investigation*

SEM-EDS investigations were performed on the $x$Na$_2$O-(100-$x$)TeO$_2$ ($0 \le x \le 33.3$ % mole fraction) glasses before and after heat treatment in order to identify changes in morphology and chemical composition. No crystals were detected by SEM in any of the investigated glasses before heat treatment. The SEM micrograph in Figure 3a for the glass containing 20.0 % mole fraction of $Na_2O$ showing homogeneous glassy phase is typical for these glasses. The EDS analysis (Figure 3b) on several different spots on glass sample gives almost identical spectra confirming homogeneous character of the sample. The chemical composition calculated from EDS spectra ($19.5 \pm 0.5$ % mole fraction of $Na_2O$ and $80.5 \pm 0.5$ % mole fraction of $TeO_2$) is in excellent agreement with nominal composition of the glass. Similar results were obtained for all investigated $Na_2O$-$TeO_2$ glasses.

The SEM investigations on $Na_2O$-$TeO_2$ glasses after the heat treatment revealed well defined crystals as shown in Figure 4a and 5a for selected samples. The SEM micrograph in Figure 4a for the crystallized glass containing 20.0 % mole fraction of $Na_2O$ shows crystalline grains with diameter of $\approx 2$ μm. EDS spectra, Figure 4b, taken from these crystalline regions have shown that crystals contain $6.4 \pm 0.5$ % mass fraction of Na, $73.0 \pm 0.5$ % mass fraction of Te and $20.6 \pm 0.5$ % mass fraction of O, which agrees well with stoichiometric composition of $Na_2Te_4O_9$ identified from XRD pattern, Figure 2.

Figure 5a shows the SEM micrograph taken from the surface of the crystallized glass containing 33.3 % mole fraction of $Na_2O$. The morphology of this sample consists of hexagonal-shaped crystals with diameter ranging from 5 to 10 μm. Based on the EDS analysis (Figure 5b), observed crystals have the same chemical composition as that of starting glass ($12.3 \pm 0.5$ % mass fraction of Na, $66.7 \pm 0.5$ % mass fraction of Te and $21.0 \pm 0.5$ % mass fraction of O) indicating crystallization of phase with $Na_2Te_2O_5$ stoichiomery. However, the XRD pattern for this crystalline phase does not match the pattern for $Na_2Te_2O_5$ available in JCPDS files, so it seems that the observed crystals correspond to a new $Na_2Te_2O_5$ polymorph.

### *Raman Spectra*

The Raman spectra of $x$Na$_2$O-(100-$x$)TeO$_2$ ($0 \le x \le 33.3$ % mole fraction) glasses are shown in Figure 6a. For all samples, spectra obtained from different spots are identical indicating high homogeneity of glasses. Each spectrum was deconvoluted and the Raman bands were assigned based on the literature data.[9,10] The most prominent band at 667 cm$^{-1}$ in the spectrum of pure $TeO_2$ glass is related to the combined vibrations of asymmetric stretching of Te–$_{eq}$O$_{ax}$–Te bonds and symmetric stretching of $TeO_4$ tbps.[9] With addition of $Na_2O$ up to 33.3 % mole fraction, intensity of this band decreases, while bands at 753 and 792 cm$^{-1}$ attributed to stretching vibrations of non-bridging Te–O$^-$ bonds in $TeO_3$ tps[10] grow in intensity. The wide band at 467 cm$^{-1}$ which de-

creases slightly with increasing $Na_2O$ content is assigned to the symmetric bending vibration of $TeO_4$ tbps and at the same time symmetric stretching vibration of $Te–_{eq}O_{ax}–Te$ linkages which are formed by vertex sharing $TeO_4$ tbps.[9,10] The very strong peak with a maximum around 40 $cm^{-1}$ observed in Raman spectra of all investigated glasses is identified as Boson peak.[22] The Boson peak is associated with light scattering due to the acoustic-like vibrations of the ordered micro-regions within the glass and the frequency can be correlated with the size of these regions. However, the spectral shape of this peak is the same for different glasses and does not normally depend on their chemical compositions.[22] The Raman results indicate that increase in $Na_2O$ content in investigated glasses results in a progressive transformation of basic structural units of $TeO_4$ tbps to $TeO_3$ tps followed by increased number of NBOs. Such a structural change associated with the formation of NBOs that

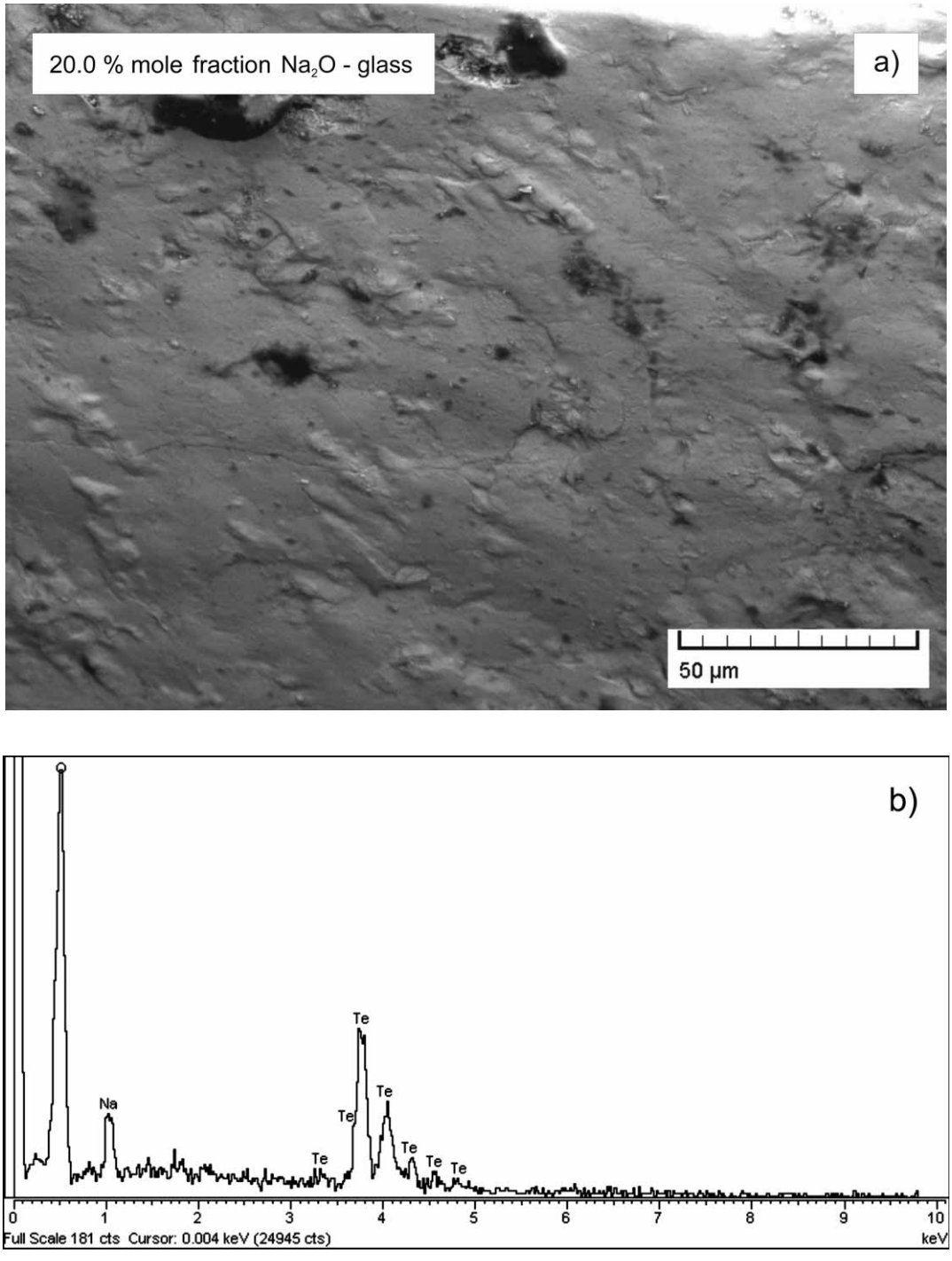


Figure 3. SEM micrograph (a) and EDS spectrum (b) of the $20.0Na_2O$-$80.0TeO_2$ % mole fraction glass.

introduce weaker ionic bonds in comparison to stronger covalent bonds (BOs), makes the glass network progressively less strong which is manifested in a decreasing $T_g$, Figure 1.

The Raman spectra for the crystallized $x$$Na_2O$-(100-$x$)$TeO_2$ ($0 \le x \le 33.3$ % mole fraction) glasses contain sharper and better defined bands as expected for crystallized material, Figure 6b. The spectrum of crystallized $TeO_2$ glass free of $Na_2O$ shows a Raman pattern typical for $\alpha$-$TeO_2$[9] which is in agreement with XRD, Figure 2. On the other hand, crystallized glasses containing 14.3, 20.0 and 25.0 % mole fraction of $Na_2O$, have almost identical spectra that also agree well with XRD showing dominant $Na_2Te_4O_9$ crystalline phase. The bands in these spectra could not be definitely assigned without further information on the crystal structures.

The structure of $\alpha$-$TeO_2$ is a three-dimensional network of corner-sharing $TeO_4$ tbps connected *via* highly

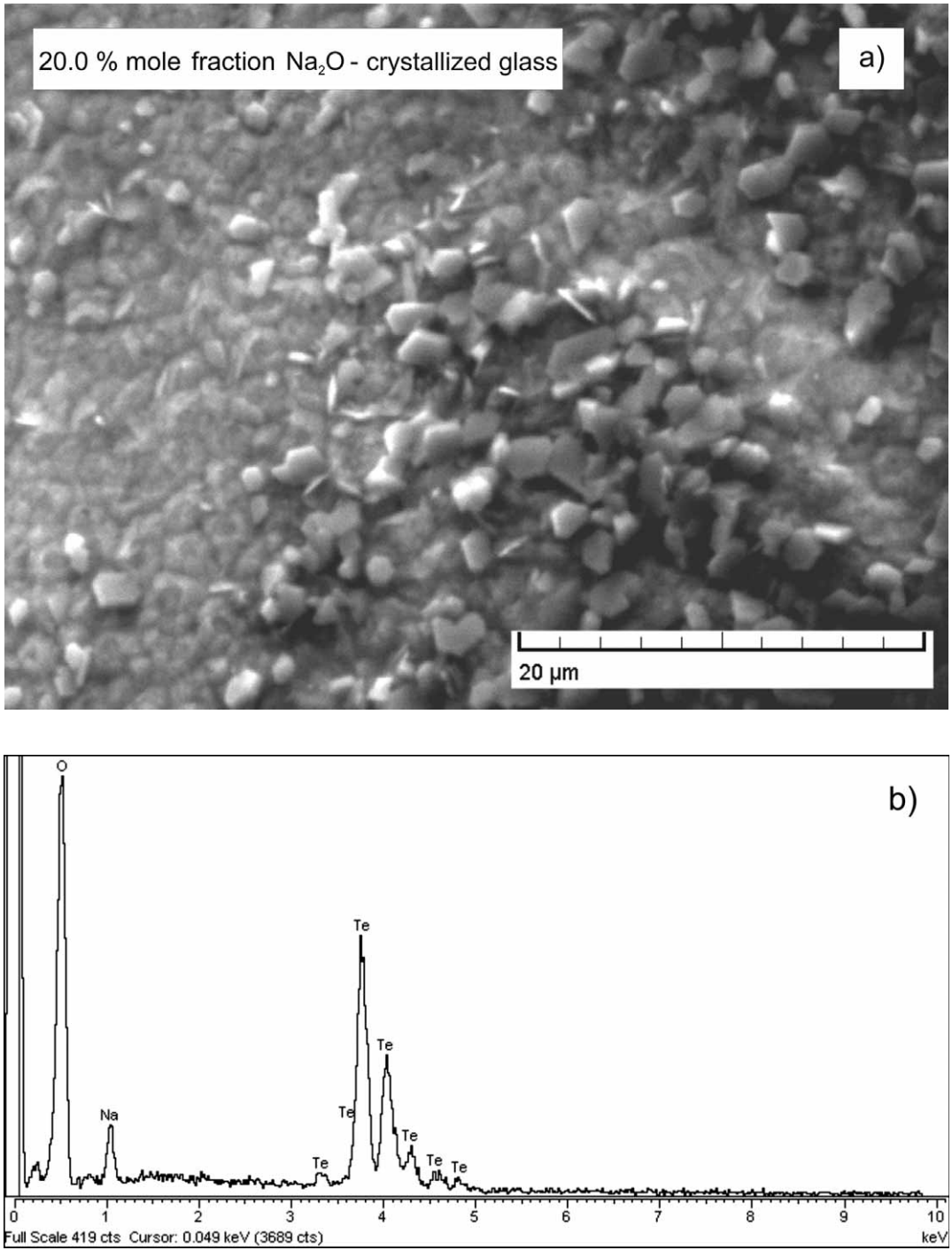


Figure 4. SEM micrograph (a) and EDS spectrum (b) of the 20.0$Na_2O$-80.0$TeO_2$ % mole fraction crystallized glass.

asymmetric Te–$_{eq}$O$_{ax}$–Te bond.[19] The Raman spectrum of $\alpha$-$TeO_2$ contains bands at 650, 396, 152, 123 and 63 $cm^{-1}$. The strongest band at 650 $cm^{-1}$ is attributed to totally symmetric stretching vibration of $TeO_4$ tbps and asymmetric stretching vibration of Te–$_{eq}$O$_{ax}$–Te bonds same as band at 667 $cm^{-1}$ in the spectrum of pure $TeO_2$ glass. The high intensity of this band results from the large difference in the polarizabilities of Te–$_{ax}$O and Te–$_{eq}$O bonds.[9] The weak band at 396 $cm^{-1}$ is related to the symmetric bending vibrations of $TeO_4$ tbps and at the same time to the symmetric stretching of the Te–$_{eq}$O$_{ax}$–Te bond.[9] The Raman bands in the low frequency region at 63, 123 and 152 $cm^{-1}$ correspond to the intra-molecular asymmetric motion of the Te–O bonds.[9]

Crystalline $Na_2Te_4O_9$ is composed of infinite $Te_4O_9^{2-}$ polymeric sheets separated by alternating layers of sodium cations.[16] Three of four tellurium atoms show typical trigonal bipyramid bonding geometries, whereas

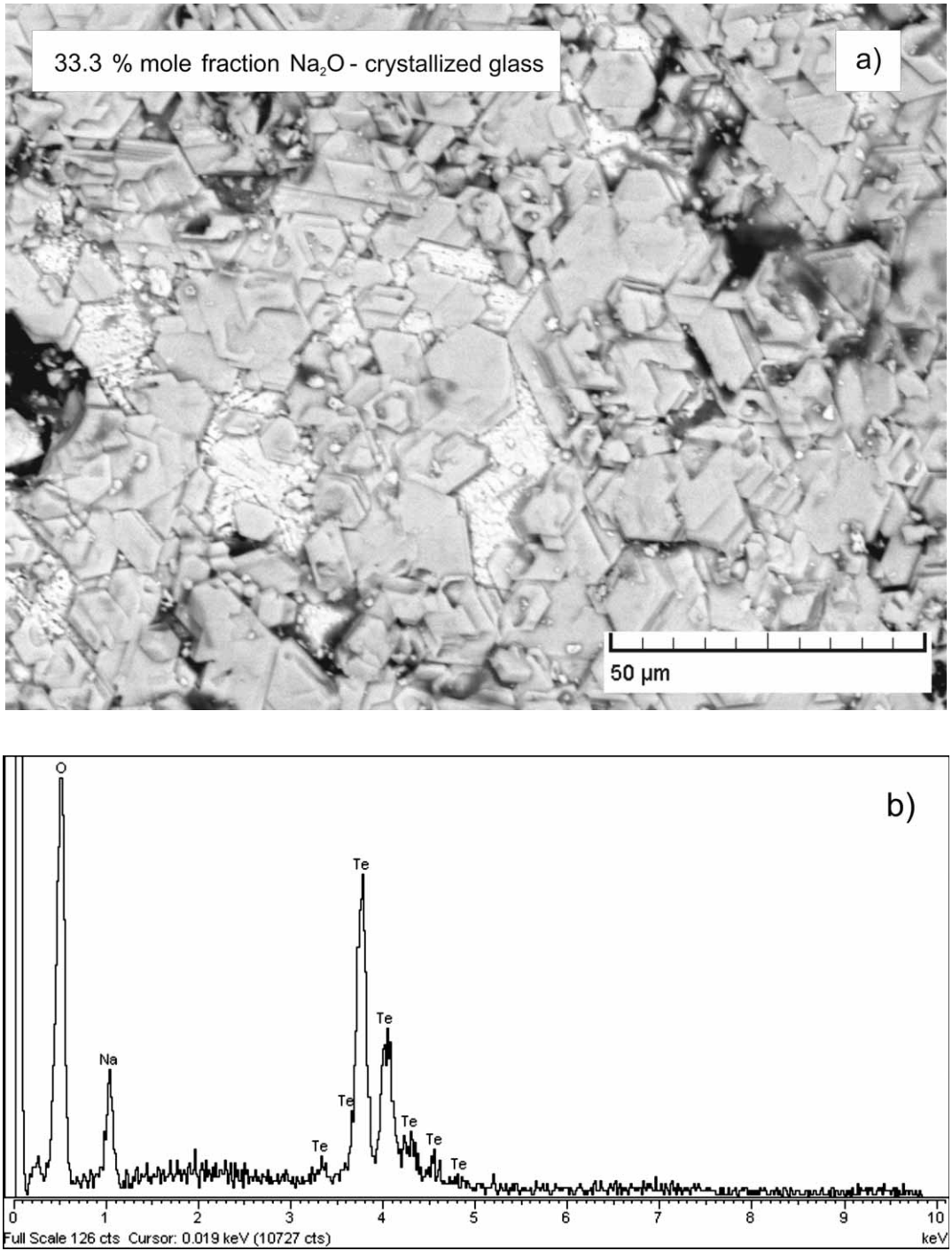


Figure 5. SEM micrograph (a) and EDS spectrum (b) of the 33.3$Na_2O$-66.7$TeO_2$ % mole fraction crystallized glass.

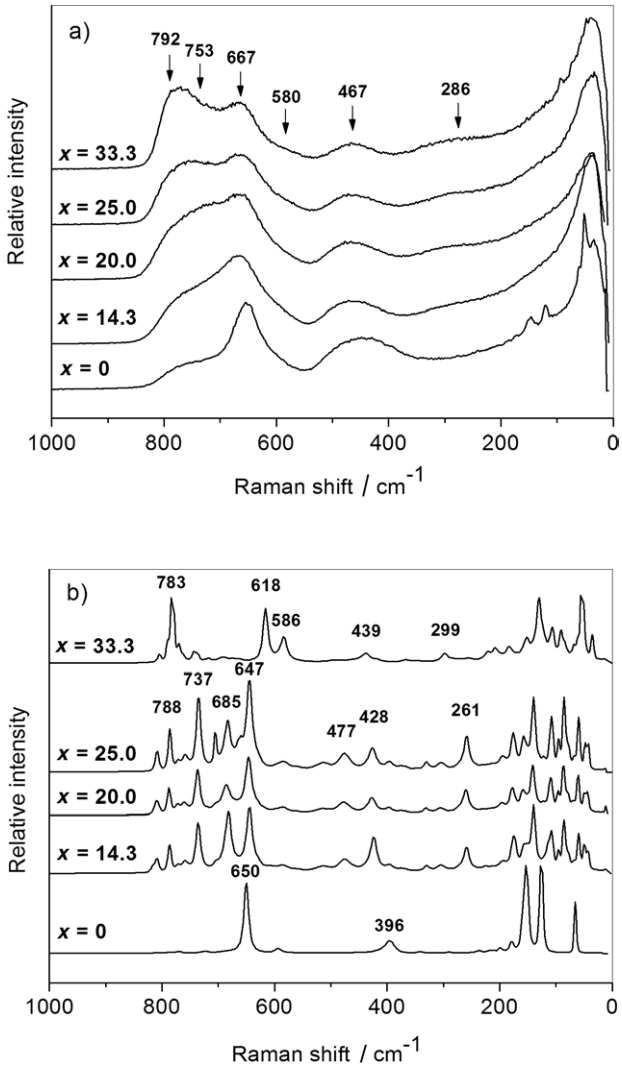


Figure 6. Raman spectra for the $x$Na$_2$O-(100-$x$)TeO$_2$ ($0 \le x \le 33.3$ % mole fraction) glasses (a) and crystallized glasses (b).

fourth tellurium atom is connected to tellurium atom from adjacent $Te_4O_9^{2-}$ units *via* two oxygen atoms in an edge sharing fashion forming $Te_2O_6$ fragments. In the Raman spectra of the crystallized glasses containing up to 25.0 % mole fraction of $Na_2O$, sharp bands are observed at 788, 737, 685, 647, 477, 428 and 261 cm$^{-1}$. The strong Raman band at 647 cm$^{-1}$ in spectra of crystallized glasses containing up to 25.0 % mole fraction of $Na_2O$ has the same origin as band at 650 cm$^{-1}$ in spectrum of $\alpha$-$TeO_2$. On the other hand, bands at 737 and 788 cm$^{-1}$ which are absent in the spectrum of $\alpha$-$TeO_2$ are related to stretching vibration of Te-O$^-$ bonds in $Te_4O_9^{2-}$ plane. The Raman bands at 477 and 428 cm$^{-1}$ are related to the symmetric vibrations of the $Te_2O_2$ double bridges from $Te_2O_6$ fragment.[23] Generally, the Raman bands in the low frequency region < 200 cm$^{-1}$ correspond to lattice modes of crystalline compound.[24] Based on the *ab initio* calculations,[24] band at 140 cm$^{-1}$ could be attributed to the rocking mode of corner sharing $TeO_4$ trigonal bypiramids and to the scissors mode of the $(TeO_2)_{eq}$ bonds.

The Raman spectrum of crystallized glass containing 33.3 % mole fraction of $Na_2O$ differs from those that contain lower $Na_2O$ content. The most prominent bands in this spectrum were observed at 783 and 618 cm$^{-1}$ along with weaker bands at 586 and 439 cm$^{-1}$. Since the diffraction peaks in XRD for this composition remain unidentified it is difficult to explain the origin of the Raman bands. However, the intense band at 783 cm$^{-1}$ which is assigned to the stretching vibration of the Te–O$^-$ bonds, suggests that the crystalline phase appeared at 33.3 % mole fraction of $Na_2O$ exhibits further cleavage of network composed of $Te_4O_9^{2-}$ polymeric sheets. The bands at 618 and 586 cm$^{-1}$ are believed to have the same origin as that for the band at 647 cm$^{-1}$ for the $x$ = 25.0 composition, and therefore, can be attributed to asymmetric vibrations of Te–O–Te bond. Like the band at 428 cm$^{-1}$ for the compositions with ≤ 25 % mole fraction of $Na_2O$, the band at 439 cm$^{-1}$ is assigned to the totally symmetric stretching vibration of the Te–O–Te bonds which are formed by sharing of $TeO_4$ tbp. The strong band at 130 cm$^{-1}$ could be assigned to rocking and scissors mode of corner sharing $TeO_4$ trigonal bypiramids similarly as band at 140 cm$^{-1}$ in spectra of compositions with ≤ 25 % mole fraction of $Na_2O$.

## CONCLUSIONS

Tellurite glasses with general formula $x$Na$_2$O-(100-$x$)TeO$_2$ were prepared by vapor deposition ($x$ = 0 % mole fraction) and melt quenching technique ($14.3 \le x \le 33.3$ % mole fraction). The structural changes of glasses and crystallized compositions obtained after the heat treatment at 623 K for 10 h in air were studied by Raman spectroscopy and XRD. The Raman spectra for the $x$Na$_2$O(100-$x$)TeO$_2$ ($0 \le x \le 33.3$ % mole fraction) glasses indicated that $TeO_4$ trigonal bypiramids (tbps) convert to $TeO_3$ trigonal pyramids (tps) with increasing $Na_2O$ content up to 33.3 % mole fraction. The XRD and Raman spectra for the crystallized compositions containing ≤ 25 % mole fraction of $Na_2O$ showed existence of known crystalline phases: $\alpha$-$TeO_2$ and $Na_2Te_4O_9$. On the other hand, glass with 33.3 % mole fraction of $Na_2O$ crystallized to unidentified phase which is believed to be new polymorph of $Na_2Te_2O_5$.

*Acknowledgements*. – The authors acknowledge Prof. V. Bermanec (Faculty of Science, Geology Department) for performing SEM and EDS analysis. This work was supported by Croatian Ministry of Science Education and Sports, projects: »Influence of structure on electrical properties of (bioactive) glasses and ceramics«, 098-0982929-2916, »Physics and applications of nanostructures and bulk matter«, 098-0982904-2898.

## REFERENCES


1. J. E. Stanworth, *Nature* **169** (1952) 581–582.
2. H. Nasu, O. Matsushita, K. Kamiya, H. Kobayashi, and K. Kubodera, *J. Non-Cryst. Solids* **124** (1990) 275–277.
3. S. H. Kim, T. Yoko, and S. Sakka, *J. Am. Ceram. Soc.* **76** (1993) 865–869.
4. D. K. Durga and N. Veeraiah, *Phys. B* **324** (2002) 127–141.
5. D. K. Durga, P. Yadagiri Reddy, and N. Veeraiah, *J. Lumin*. **99** (2002) 53–60.
6. A. A. Bahgat, E. E. Shaisha, and A. I. Sabry, *J. Mater. Sci.* **22** (1987) 1323–1327.
7. D. Zhu, C. S. Ray, W. Zhou and D. E. Day, *J. Mater. Sci.* **39** (2004) 7351–7357.
8. S. L. Tagg, R. E. Youngman, and J. W. Zwanziger, *J. Phys. Chem.* **99** (1995) 5111–5116.
9. T. Sekiya, N. Mochida, A. Ohtsuka, and M. Tonokawa, *J. Ceram. Soc. Jpn* **97** (1989) 1435–1440.
10. T. Sekiya, N. Mochida, A. Ohtsuka, and M. Tonokawa, *J. Non-Cryst. Solids* **144** (1992) 128–144.
11. J. Heo, D. Lam, G. H. Sigel Jr., E. A. Mendoza, and D. A. Hensley, *J. Am. Ceram. Soc.* **75** (1992) 227–281.
12. S. Sakida, S. Hayakawa, and T. Yoko, *J. Non-Cryst. Solids* **243** (1999) 1–12.
13. S. Sakida, S. Hayakawa, and T. Yoko, *J. Non-Cryst. Solids* **243** (1999) 13–25.
14. J. C. McLaughlin, S. L. Tagg, J. W. Zwanziger, D. R. Haeffner, and S. D. Shastri, *J. Non-Cryst. Solids* **274** (2000) 1–8.
15. J. C. McLaughlin, S. L. Tagg, and J. W. Zwanziger, *J. Phys. Chem. B.* **105** (2001) 67–75.
16. J. W. Zwanziger, J. C. McLaughlin, and S. L. Tagg, *Phys. Rev. B* **56** (1997) 5243–5249.
17. T. Uchino and T. Yoko, *J. Non-Cryst. Solids* **204** (1996) 243–252.
18. D. Holland, J. Bailey, G. Ward, B. Turner, P. Tierney, and R. Dupree, *Solid State Nucl. Magn. Reson.* **27** (2005) 16–27.
19. S. L. Tagg, J. C. Huffman, and J. W. Zwanziger, *Chem. Mater.* **6** (1994) 1884–1889.
20. S. L. Tagg, J. C. Huffman, and J. W. Zwanziger, *Acta Chem. Scand.* **51** (1997) 118–121.
21. C. S. Ray and D. E. Day, *Ceram. Trans.* **30** (1993) 207–221.
22. G. S. Murugan and Y. Ohishi, *J. Non-Cryst. Solids* **351** (2005) 364–371.
23. A. P. Mirgorodsky, T. Merle-Mejean, J. C. Champarnaud, P. Thomas, and B. Frit, *J. Phys. Chem. Solids* **61** (2000) 501–509.
24. T. A. Mohamed, I. Shaltout, and K. M. Al Yahyaei, *Spectrochim. Acta, Part A* **64** (2006) 106–115.


---

## SAŽETAK

### Strukturna svojstva i kristalizacija natrijskih teluritnih stakala

**Ana Šantić, Andrea Moguš-Milanković, Krešimir Furić, Maša Rajić-Linarić, Chandra S. Ray i Delbert E. Day**

Strukturna svojstva i kristalizacija $x$Na$_2$O-(100-$x$)TeO$_2$ ($0 \le x \le 33.3$, $x$-% molnog udjela) stakala istraživana su Ramanskom spektroskopijom, difrakcijskom rentgenskom analizom (XRD) i diferencijskom pretražnom kalorimetrijom (DSC). Ramanski spektri stakala pokazali su sistematsku promjenu strukturnih jedinica, od TeO$_4$ trigonskih bipiramida (tbps) do TeO$_3$ trigonskih piramida (tps) s povećanjem udjela Na$_2$O u staklima. Strukturne promjene nastale povećanjem udjela Na$_2$O posljedica su pucanja Te–$_{eq}$O$_{ax}$–Te veza i nastajanja nepremoščujućih atoma kisika (NBOs) u strukturnoj mreži stakla. Grijanjem stakala na 623 K u periodu od 10 h kristaliziraju različite faze: $\alpha$-TeO$_2$, Na$_2$Te$_4$O$_9$ i nova kristalna faza koja je vjerojatno polimorf Na$_2$Te$_2$O$_5$.